

# Laser-induced thermal emission of carbon microparticles on transparent heat-sink substrates

K.S. Zelenska<sup>1</sup>, S.E. Zelensky<sup>1\*</sup>, O.S. Kolesnik<sup>1</sup>, Toru Aoki<sup>2</sup>, P.O. Teselko<sup>1</sup>

<sup>1</sup>Taras Shevchenko National University of Kyiv, Faculty of Physics  
64/13, Volodymyrska str., 01601 Kyiv, Ukraine

<sup>2</sup>Research Institute of Electronics, Shizuoka University  
Johoku 3-5-1, Naka-ku, Hamamatsu 432-8011, Japan

\*Corresponding author e-mail: Zelensky@knu.ua

**Abstract.** Thermal emission is an informative tool to study materials' properties at high temperatures under laser irradiation. The kinetics decay of laser-induced thermal emission from carbon microparticles deposited on heat-sink surfaces of transparent dielectrics (glass and sapphire) was studied. A Q-switched YAG:Nd<sup>3+</sup> laser (pulse duration  $\tau_i = 20$  ns, energy/power density  $0.5 \text{ J}\cdot\text{cm}^{-2}$ ,  $25 \text{ MW}\cdot\text{cm}^{-2}$ ) was employed to excite thermal emission. In calculations, the classical heat conduction equation was used. With increasing the thermal conductivity of substrate (from glass to sapphire), reduction in the emission pulse duration has been observed.

**Keywords:** laser-induced thermal emission, carbon microparticles, heat-sink substrate.

<https://doi.org/10.15407/spqeo26.02.201>

PACS 42.62.-b, 44.40.+a

Manuscript received 10.05.23; revised version received 20.05.23; accepted for publication 07.06.23; published online 26.06.23.

## 1. Introduction

Under illumination of light-absorbing materials with pulsed or modulated laser radiation, the laser-induced changes of temperature cause the appropriate increase of thermal emission of the irradiated material. Properties of this laser-induced thermal emission are dependent on thermal and optical characteristics of the irradiated material, and a group of methods called photothermal radiometry [1–5] was elaborated. In [1–5], local increase of temperature can be of the order of dozens of Kelvins, and the corresponding thermal emission is usually detected in the IR spectral region. With the use of high-power pulsed lasers, local temperature can reach thousands of Kelvins [6], and this laser-induced thermal emission can be easily detected in the visible spectral region. For such emission, high-sensitive and high-speed photomultiplier detectors can be used, and this circumstance opens good opportunities to study relatively fast processes in the nanosecond and sub-microsecond time scale. For example, short pulses of visible thermal emission (with the pulse length of  $10^{-8}$  to  $10^{-7}$  s) can be observed when surface layers of light-absorbing materials are heated up by nanosecond laser pulses. This pulsed thermal emission can provide information about material's properties at high temperatures and about the processes of laser radiation interaction with matter [7–13]. As shown in [7, 8, 11], the decay of thermal emission

after pulsed laser excitation depends on the relationship between thermal and optical characteristics of the irradiated material, as well as on the geometry of heat release region. In particular, laser radiation penetration depth into the irradiated material,  $\Delta$ , and thermal diffusion length during typical time of the studied processes,  $\delta$ , are the parameters which define the decay of laser-induced thermal emission. If  $\Delta > \delta$ , trailing edges of pulsed signals of laser-induced thermal emission contain slow decay components (of the order of  $10^{-7}$  s), which can be easily detected under excitation with radiation of typical Q-switched lasers.

In the case of rough surface layers, decay kinetics of laser-induced thermal emission depends not only on the ratio  $\Delta/\delta$  but also on the dimensions of the elements of rough surface relief [8].

Numerous papers consider visible thermal emission of light-absorbing microparticles heated up with nanosecond laser pulses. In particular, thermal emission was studied using carbon microparticles suspended in various matrices: aerosols [14–16], aqueous suspensions [17–20], glass [21, 22], and transparent polymers [23, 24]. Depending on chemical composition of the matrix, thermal emission of carbon microparticles under pulsed laser heating have different properties due to variety of processes of the laser energy transformation in the microparticles and in the surrounding matrix.

This paper is devoted to studies of kinetics decay inherent to thermal emission of carbon microparticles deposited on surfaces of transparent dielectrics. It is supposed that the distribution of temperature inside microparticles under the laser irradiation will be affected by heat dissipation into the substrate material transparent for the laser light. Then, according to the mechanism of formation of slow components in the decay of laser-induced thermal emission [7, 8], it is expected that the substrate-induced changes of temperature distribution will cause considerable shortening of the decay curves.

## 2. Methods

To excite thermal emission of carbon microparticles, a Q-switched YAG:Nd<sup>3+</sup> laser was employed (pulse duration  $\tau_i = 20$  ns, energy and power density approximately  $0.5 \text{ J}\cdot\text{cm}^{-2}$  and  $25 \text{ MW}\cdot\text{cm}^{-2}$ ). The measurements were performed in a single shot mode at room temperature. Laser-induced thermal emission was detected with a photomultiplier Hamamatsu H1949-51 (rise time 1.3 ns) through a blue glass optical filter CC-4 (bandwidth 400...500 nm). The signals were analyzed with a digital oscilloscope TDS2022B (bandwidth 200 MHz).

Carbon microparticles were deposited on polished surfaces of glass and sapphire samples. Deposition was made using laser ablation at atmospheric pressure. A carbon-containing target (carbon-filled paper) was irradiated with 1-3 laser pulses ( $0.5 \text{ J}\cdot\text{cm}^{-2}$ ,  $25 \text{ MW}\cdot\text{cm}^{-2}$ ). The distance between the target and substrate was approximately 4 mm. Typical SEM images of the deposited particles are given in Fig. 1.

The calculations were carried out similarly to [7]. Since the surface temperature reaches several thousands of degrees, the calculations require high-temperature data

on thermal and optical characteristics of the irradiated material. A large number of studies were devoted to measuring the thermal conductivity of carbon materials, and a comprehensive review is given in [25]. However, for temperature range  $>1000 \text{ K}$ , the data given in [25] are not so numerous. In the present work, we follow the conclusions obtained in [7], and for carbon we use the high-temperature estimate of thermal conductivity coefficient  $\kappa = 0.04 \text{ W}\cdot\text{m}^{-1}\cdot\text{K}^{-1}$ , the specific heat capacity  $c_p = 4\cdot 10^6 \text{ J}\cdot\text{m}^{-3}\cdot\text{K}^{-1}$ , and the absorption coefficient  $\alpha = 10^7 \text{ m}^{-1}$  (at the laser wavelength of 1064 nm). For thermal characteristics of the substrate materials, the following values are assumed:  $\kappa = 1 \text{ W}\cdot\text{m}^{-1}\cdot\text{K}^{-1}$ ,  $c_p = 2.15\cdot 10^6 \text{ J}\cdot\text{m}^{-3}\cdot\text{K}^{-1}$ , and  $\kappa = 27 \text{ W}\cdot\text{m}^{-1}\cdot\text{K}^{-1}$ ,  $c_p = 1.66\cdot 10^6 \text{ J}\cdot\text{m}^{-3}\cdot\text{K}^{-1}$ , which roughly corresponds to typical values for silicate glass and sapphire, respectively [26]. In all of the calculations, the dependence of the thermal and optical characteristics on temperature and on the intensity of laser radiation was neglected.

## 3. Results and discussion

In the experiments, the laser pulses irradiated the particles from the side opposite to the place of their contact with the heat sink substrate. To simulate temperature distribution inside a single particle, the following one-dimensional model was used (see Fig. 2): a layer of carbon with a thickness  $h$  covers a flat surface of substrate, and the laser radiation propagates in the direction of  $z$ -axis, perpendicularly to the substrate surface.

The laser intensity was presented by the following expression  $F(z, t) = F_0(z) \varphi(t)$ , where function  $\varphi(t)$  describes the shape of the laser pulse, and function  $F_0(z)$  describes its attenuation along  $z$ -axis. In the calculations, we used two versions of the laser pulse shape: rectangular and Gaussian.

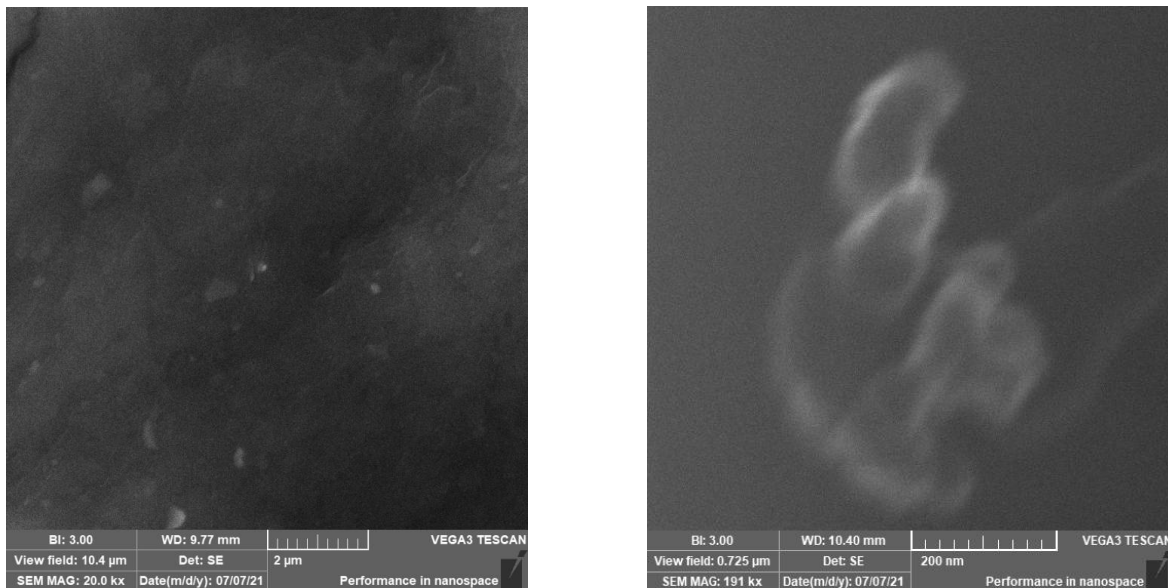
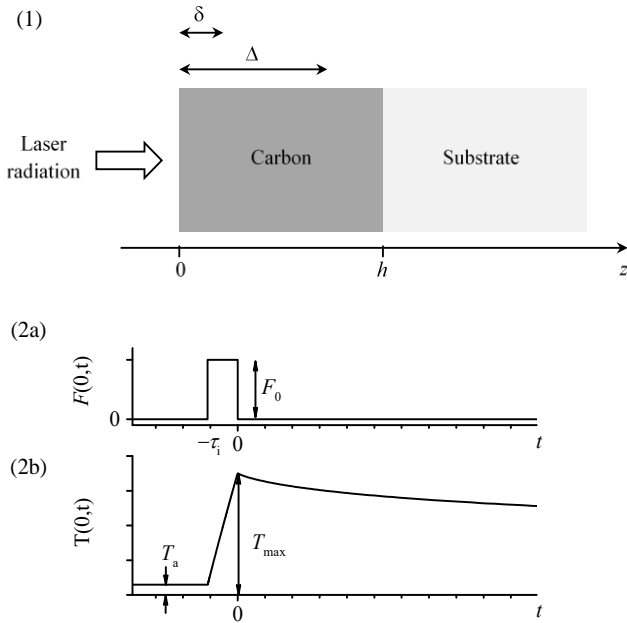


Fig. 1. SEM images of a polished Si surface with deposited carbon microparticles.



**Fig. 2.** The sample geometry for computations (1) and typical oscillograms of a rectangular laser pulse (2a) and temperature (2b) at  $z = 0$ .

Absorption of laser radiation was described by the following equation:

$$dF_0 = -\alpha F dz. \quad (1)$$

The penetration depth of laser radiation into the carbon material was estimated as  $\Delta = \alpha^{-1} = 100$  nm. For the substrate material, zero absorption coefficient was assigned. Reflections at the interfaces were neglected.

Transient temperature distribution was calculated using the parabolic heat conduction equation:

$$\frac{\partial}{\partial z} \kappa \frac{\partial}{\partial z} T + \alpha F = c_p \frac{\partial}{\partial t} T. \quad (2)$$

Heat dissipation to the surrounding atmosphere was neglected. The object temperature before irradiation was taken equal to room temperature  $T(z, t < 0) = T_a = 293$  K. The thermal diffusion length  $\delta$  in carbon was estimated

$$\text{as } \delta = \sqrt{\frac{\kappa}{c_p} \tau_i} \approx 14 \text{ nm}.$$

The surface exitance  $\varepsilon$  in a narrow spectral interval  $(\lambda, \lambda + \Delta\lambda)$ , where  $\lambda = 450$  nm and  $\Delta\lambda = 1$  nm, was calculated with the use of Planck's blackbody emission law with the surface temperature  $T(z = 0, t)$  calculated from Eqs (1) and (2).

For laser-induced thermal emission (Fig. 2), the decay starts at  $t = 0$ , and the decay curve  $\varepsilon(t)$  at  $t > 0$  is determined by the kinetics of temperature at  $z = 0$ . In its turn, the decay kinetics of  $T(z = 0, t > 0)$  depends not only on thermal characteristics of the irradiated material,

but also on the initial distribution of temperature at the moment of the onset of decay  $T(z, t = 0) = T_{\max}(z)$ . Here two cases should be considered.

First, in the case of  $\Delta < \delta$ , the heat release region is of the order of  $\Delta$ , and the depth of the initial distribution of temperature  $T_{\max}(z)$  is of the order of  $\delta$ . In this case, the emission decay time reaches dozens of nanoseconds [7].

Second, in the case of  $\Delta > \delta$  the power of internal heat source decreases rather smoothly with  $z$  (in accordance with Eq. (1)). As a result, at  $t = 0$ , the temperature gradient  $dT_{\max}/dz$  is relatively small; hence, the slow component appears in the emission decay.

For carbon particles deposited on a flat surface, according to the model presented in Fig. 2 (1), for  $h$  of the order of  $\Delta$ , the presence of heat-conducting substrate can change the initial distribution of temperature  $T_{\max}(z)$ . As a result, changes of the laser-induced thermal emission decay curves can be expected.

The calculated initial temperature distributions  $T_{\max}(z)$  are shown in Fig. 3 for different values of thicknesses  $h$ . As seen from the figure, the presence of heat-sink substrate changes the temperature distribution significantly. When the particle is in contact with the heat sink surface, the outflow of thermal energy into the substrate affects the temperature distribution in the part of the microparticle adjacent to the substrate. This is clearly seen in Fig. 3: temperature decreases noticeably within the layer  $(h - \delta, h)$ . If the particle size is small, the distortion of the temperature distribution in the region  $(h - \delta, h)$  can affect the temperature gradient in the region  $(0, \delta)$ ; hence, the emission decay kinetics can change.

Calculated oscillograms (time histories) of the surface exitance are given in Fig. 4 for different  $h$  under excitation by rectangular laser pulses. Similarly to [7], the decay curves given in Fig. 4 demonstrate a combination of fast ( $10^{-8}$  s) and slow ( $10^{-7}$  s) decay components.

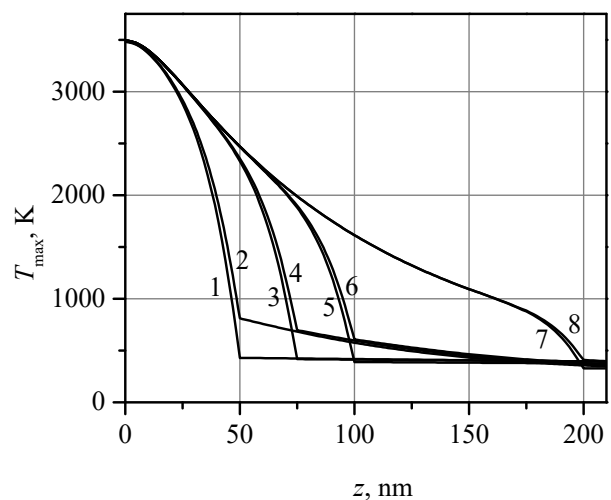


**Fig. 3.** Maximal temperature  $T_{\max}$  as a function of  $z$  for  $h = 50$  nm (1, 2), 75 nm (3, 4), 100 nm (5, 6), 200 nm (7, 8) for sapphire (1, 3, 5, 7) and glass substrate (2, 4, 6, 8).

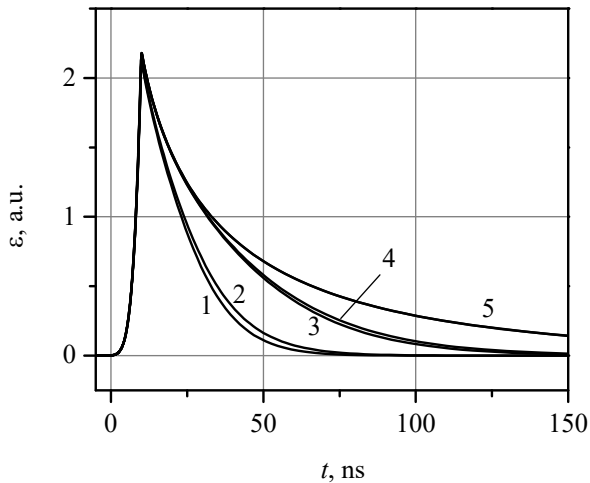


**Fig. 4.** Oscillograms of thermal radiation for  $h = 50$  nm (1, 2), 75 (3, 4), 150 (5) for sapphire (1, 3, 5) and glass substrate (2, 4, 5).

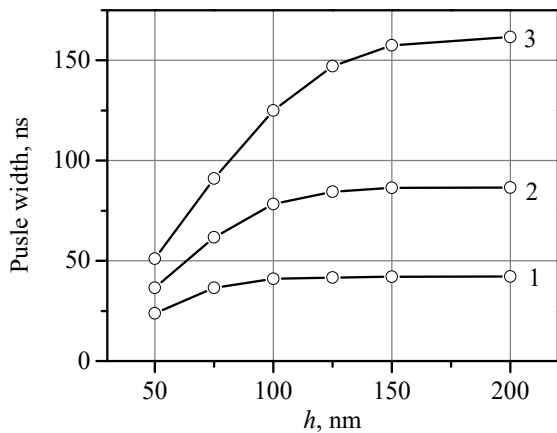


**Fig. 5.** The emission pulse duration as a function of  $h$  on the glass substrate at the levels 0.5 (1), 0.25 (2), 0.1 (3).

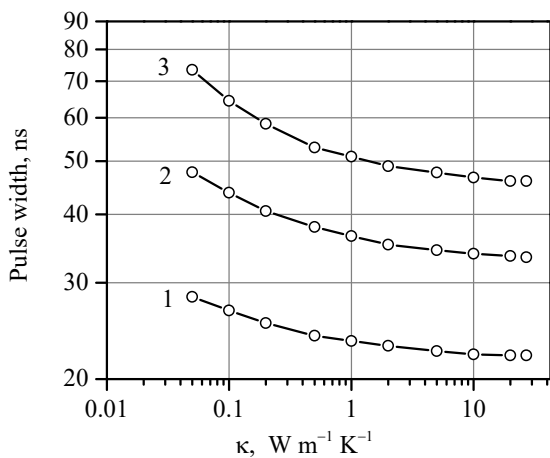


**Fig. 6.** The emission pulse duration as a function of thermal conductivity of the substrate at the levels 0.5 (1), 0.25 (2), 0.1 (3).

As mentioned above, the shape of emission decay curve depends on many factors, and its approximation is a complicated task. In the case of  $\Delta > \delta$  for flat surfaces of uniform materials, as shown in [7], the emission decay curve can be approximately fitted by a double-exponent function (at least in a limited range of the emission intensity). In the case of microparticles deposited on substrates, approximation of the calculated emission decay curves by a sum of two exponentials leads to unsatisfactory results, especially for small particle sizes  $h \leq 3\delta$ . Therefore, in this work, the double-exponent approximation is not used.

As seen from Fig. 3, with the decrease of  $h$  the carbon-glass interface comes closer to the irradiated surface, and it leads to a noticeable change in the temperature distribution in the near-surface region. Since thermal conductivity of the substrate material is significantly higher than that of carbon, the decrease of  $h$  leads to the increase of temperature gradient near the irradiated surface, which in its turn leads to the change of shape of the emission decay curve. As can be seen from Fig. 4, for small values of  $h$ , the slow component of the emission decay disappears (curves 1, 2 in Fig. 4).

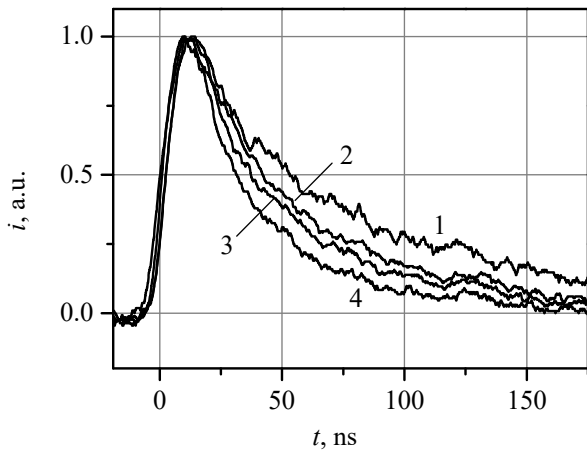
It should be noted that the shape of the laser pulses used in the measurements in this work is far from rectangular. As shown in [7], the non-rectangularity of the laser pulse shape can significantly affect the emission decay curve, especially in its fast stage. Therefore, hereinafter we consider the results of calculations with Gaussian laser pulses for comparison of the calculated and experimental data. It also should be noted, there is a significant delay between the maximum of the laser pulse and the maximum of the emission oscillogram.

Now consider the influence of characteristics of the irradiated objects on the duration of the emission pulsed signals. Since the emission pulse has a complex trailing edge with a slow decay component, we analyze the pulse duration at a level of 0.5, 0.25, and 0.1 of its maximal value.

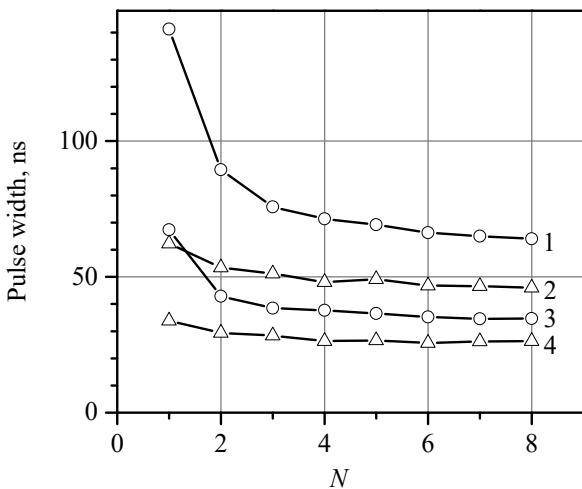
Fig. 5 shows the calculated pulse width as a function of  $h$ . As seen from the figure, the decrease of  $h$  leads to significant reduction in the duration of the emission pulse signal.

Fig. 6 shows the calculated dependences of the emission pulse width on the value of thermal conductivity of the substrate material for  $h = 50$  nm. As seen from the figure, the calculations predict noticeable changes in the width of emission pulses caused by variations of thermal conductivity of substrates, and these changes are more pronounced, when the pulse duration is measured at the level 0.1.

Typical normalized experimental emission oscillograms are shown in Fig. 7. The oscillograms were recorded when the sample was irradiated by a sequence of identical laser pulses with the interval close to 30 s. The pulse number in the sequence is designated as  $N$ . As seen from the figure, the shape of the emission pulse changes with increasing  $N$ .



**Fig. 7.** Normalized oscillograms of thermal emission typical to carbon microparticles on the glass substrate for  $N = 1$  (1), 2 (2), 3 (3), 10 (4).



**Fig. 8.** The duration of thermal emission pulses (at the levels 0.25 (1, 2) and 0.5 (3, 4)) as a function of pulse number  $N$  for carbon microparticles on the glass (1, 3) and sapphire substrate (2, 4).

Fig. 8 shows the experimental data on the duration of thermal emission pulses for carbon microparticles on the glass and sapphire substrates. The data for pulse width at the level 0.1 are not considered due to the significant errors caused by noise in the oscillograms.

As it can be seen from Fig. 8, the emission pulse width depends on the type of substrate: for the sapphire substrate the pulse duration is significantly shorter than for the glass substrate.

The results shown in Fig. 8 are in qualitative agreement with the above-described results of computer simulations. With the increase of thermal conductivity of the substrate (from glass to sapphire), 25...55% reduction in the emission pulse duration is observed in the experiment (Fig. 8), while calculations predict much smaller reduction of 6...9% (Fig. 6). This circumstance additionally shows the limitations of the model used in

the calculations. It should be noted that the employed model uses a number of approximations, both specified above in the text and not mentioned. For example, the model does not take into account the thermal resistance in the carbon-substrate interface. Besides, the contact area of the particle with the substrate may differ from the area of the irradiated particle surface. Nevertheless, despite the limitations, for pulsed laser heating of microparticles on heat-sink substrates, the considered model clarifies the mechanism of formation of thermal emission signals and predicts noticeable reduction of the emission pulse width.

#### 4. Concluding remarks

The above presented results of measurements and calculations indicate a noticeable effect of the substrate on the decay kinetics of laser-induced thermal emission of carbon microparticles: the presence of a heat-dissipating substrate causes significant reduction of the emission pulse duration. This circumstance opens possibilities for using such particles as a probe for monitoring thermal conductivity of surface layers of transparent materials. Besides, being based on the considered model, it can be predicted that the decay kinetics can be sensitive to the presence of local absorption of laser radiation in the surface layer of the substrate. Finally, it also should be noted that the considered approach can be used for analysis of pulsed laser-induced thermal emission of thin films on heat sink substrates.

#### Acknowledgements

This research was partly supported by 2021 Cooperative Research at Research Center of Biomedical Engineering, Japan, adopted as 2021 Cooperative Research at RIE, Shizuoka University (Grant No. 2065), and by the Ministry of Education and Science of Ukraine in accordance with Agreement No. BF/30-2021 dated August 4, 2021 with TSNUK.

#### References

1. Fomina P.S., Proskurnin M.A. Photothermal radiometry methods in materials science and applied chemical research. *J. Appl. Phys.* 2022. **132**. P. 040701. <https://doi.org/10.1063/5.0088817>.
2. Battaglia J.-L., Ruffio E., Kusiak A. *et al.* The periodic pulse photothermal radiometry technique within the front face configuration. *Measurement*. 2020. **158**. P. 107691. <https://doi.org/10.1016/j.measurement.2020.107691>.hal-02998129.
3. Xiao P. Photothermal radiometry for skin research. *Cosmetics*. 2016. **3**, No 1. P. 10. <https://doi.org/10.3390/cosmetics3010010>.
4. Fleurence N., Hay B., Davee G. *et al.* Thermal conductivity measurements of thin films at high temperature modulated photo-thermal radiometry at LNE. *phys. status solidi (a)*. 2015. **212**. P. 535–540. <https://doi.org/10.1002/pssa.201400084>.

5. Mikulewitsch M., Ströbel G., Fischer A. *et al.* Influences on quantitative nitriding layer thickness measurements using model-based photothermal radiometry. *HTM J. Heat Treat. Mater.* 2022. **77**, No 5. P. 357–373. <https://doi.org/10.1515/htm-2022-1024>.
6. Zelensky S.E., Zelenska K.S. Laser-induced incandescence of carbon surface: a method for temperature estimation. *Nonlinear Optics and Applications VII.* 2013. **8772**. P. 226–233. <https://doi.org/10.1117/12.2017091>.
7. Zelensky S.E., Aoki T. Decay kinetics of thermal emission of surface layers of carbon materials under pulsed laser excitation. *Opt. Spectrosc.* 2019. **127**. P. 858. <https://doi.org/10.1134/S0030400X19110298>.
8. Karpovych V., Tkach O., Zelenska K., Zelensky S., Aoki T. Laser-induced thermal emission of rough carbon surfaces. *J. Laser Appl.* 2020. **32**. P. 012010. <https://doi.org/10.2351/1.5131189>.
9. Zelenska K.S., Zelensky S.E., Kopyshinsky A.V., Rozouvan S.G., Aoki T. Laser-induced incandescence of rough carbon surfaces. *Jpn. J. Appl. Phys.: Conf. Proc.* 2016. **4**. P. 011106–1–6. <https://doi.org/10.7567/JJAPCP.4.011106>.
10. Zelensky S.E., Poperenko L.V., Kopyshinsky A.V., Zelenska K.S. Nonlinear characteristics of laser-induced incandescence of rough carbon surfaces. *Proc. SPIE.* 2012. **8434**. P. 8434H–1–6. <https://doi.org/10.1117/12.921999>.
11. Zelenska K., Zelensky S., Kopyshinsky A. Effect of thermal conductivity of carbon superficial layers on the kinetics of laser-induced incandescence. *Thai J. Nanosci. Nanotechnol.* 2017. **2**. P. 1–8.
12. Kokhan M., Koleshnia I., Zelensky S., Hayakawa Y., Aoki T. Laser-induced incandescence of GaSb/InGaSb surface layers. *Opt. Laser Technol.* 2018. **108**. P. 150–154. <https://doi.org/10.1016/j.optlastec.2018.06.053>.
13. Kopyshinsky A.V., Zelensky S.E., Gomon E.A., Rozouvan S.G., Kolesnik A.S. Laser-induced incandescence of silicon surface under 1064-nm excitation. *SPQEO.* 2012. **15**. P. 376–381. <https://doi.org/10.15407/spqeo15.04.376>.
14. Michelsen H.A., Schulz C., Smallwood G.J., Will S. Laser-induced incandescence: Particulate diagnostics for combustion, atmospheric, and industrial applications. *Prog. Energy Combust. Sci.* 2015. **51**. P. 2–48. <https://doi.org/10.1016/j.pecs.2015.07.001>.
15. Zhang Y., Liu F., Clavel D. *et al.* Measurement of soot volume fraction and primary particle diameter in oxygen enriched ethylene diffusion flames using the laser-induced incandescence technique. *Energy.* 2019. **177**. P. 421–432. <https://doi.org/10.1016/j.energy.2019.04.062>.
16. Sipkens T.A., Menser J., Dreier T. *et al.* Laser-induced incandescence for non-soot nanoparticles: recent trends and current challenges. *Appl. Phys. B* 2022. **128**. P. 72. <https://doi.org/10.1007/s00340-022-07769-z>.
17. Zelensky S. Laser-induced heat radiation of suspended particles: a method for temperature estimation. *J. Opt. A: Pure Appl. Opt.* 1999. **1**. P. 454–458. <https://doi.org/10.1088/1464-4258/1/4/306>.
18. Zelensky S. Laser-induced incandescence of suspended particles as a source of excitation of dye luminescence. *J. Lumin.* 2003. **104**. P. 27–33. [https://doi.org/10.1016/S0022-2313\(02\)00661-0](https://doi.org/10.1016/S0022-2313(02)00661-0).
19. Rulik Ju.Ju., Mikhailenko N.M., Zelensky S.E., Kolesnik A.S. Laser-induced incandescence in aqueous carbon black suspensions: the role of particle vaporization. *SPQEO.* 2007. **10**. P. 6–10. <https://doi.org/10.15407/spqeo10.01.006>.
20. Zelensky S.E., Kolesnik A.S., Kopyshinsky A.V. Vaporization of carbon in aqueous suspensions under pulsed laser irradiation. *Ukr. J. Phys.* 2007. **52**. P. 946–950.
21. Zelensky S. Laser-induced heat radiation in borate glass. *J. Condens. Matter Phys.* 1998. **10**. P. 7267–7272. <https://doi.org/10.1088/0953-8984/10/32/017>.
22. Kopyshinsky A.V., Lazorenko Ya.P., Zelensky S.E. Laser-induced incandescence of borate glass doped with carbon microparticles. *Funct. Mater.* 2011. **18**. P. 116–120.
23. Zelensky S.E., Kolesnik A.S., Kopyshinsky A.V. *et al.* Thermal emission of carbon microparticles in polymer matrices under pulsed laser excitation. *Ukr. J. Phys.* 2009. **54**. P. 983–988.
24. Zelenska K.S., Zelensky S.E., Poperenko L.V. *et al.* Thermal mechanisms of laser marking in transparent polymers with light-absorbing microparticles. *Opt. Laser Technol.* 2016. **76**. P. 96–100. <https://doi.org/10.1016/j.optlastec.2015.07.011>.
25. Ho C.Y., Powell R.W., Liley P.E. Thermal conductivity of the elements: A comprehensive review. *J. Phys. Chem. Ref. Data, Suppl.* 1974. **3**, No 1. P. 1–796.
26. *International Critical Tables of Numerical Data, Physics, Chemistry and Technology.* First Electronic Edition. Ed. E.W. Washburn. Norwich, New York, 2003.

#### Authors' contributions

**Kateryna Zelenska:** investigation, writing – original draft, visualization, writing – review & editing.

**Serge Zelensky:** conceptualization, methodology, software, writing – review & editing, project administration.

**Olexandr Kolesnik:** investigation, resources, formal analysis.

**Toru Aoki:** conceptualization, methodology, project administration, funding acquisition.

**Peter Teselko:** investigation, visualization, formal analysis.

## Authors and CV

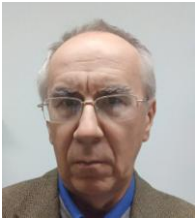


**Kateryna Zelenska**, PhD, Research Fellow at the Faculty of Physics, Taras Shevchenko National University of Kyiv, Ukraine. Authored over 30 scientific publications. The area of her scientific interests includes laser spectroscopy, laser induced thermal emission, THz spectroscopy, liquid-

liquid phase separation, semiconductor physics.

E-mail: [czelenska@gmail.com](mailto:czelenska@gmail.com),

<https://orcid.org/0000-0001-5500-8796>



**Serge Zelensky**, DSc, Professor, Vice-Dean of the Faculty of Physics, Taras Shevchenko National University of Kyiv, Ukraine. Authored over 90 scientific and educational publications. The area of his scientific interests includes optics, laser-matter interactions, luminescence.

<https://orcid.org/0000-0001-8545-6784>



**Olexandr Kolesnik**, Senior Engineer at the Faculty of Physics, Taras Shevchenko National University of Kyiv, Ukraine. Authored over 10 scientific publications. The area of his scientific interests includes lasers and electronics.

E-mail: [oskol@univ.kiev.ua](mailto:oskol@univ.kiev.ua)



**Toru Aoki**, PhD, Professor, Deputy Director at the Research Institute of Electronics, Shizuoka University, Hamamatsu, Shizuoka, Japan. Authored over 300 scientific publications. The area of his scientific interests includes radiation detectors and imaging, medical photonics,

nanovision science, photon counting X-ray CT, doping of semiconductors.

E-mail: [aoki.toru@shizuoka.ac.jp](mailto:aoki.toru@shizuoka.ac.jp),

<https://orcid.org/0000-0002-6107-3962>



**Peter Teselko**, PhD, Research Fellow at the Faculty of Physics, Taras Shevchenko National University of Kyiv, Ukraine. Authored over 50 scientific publications. The area of his scientific interests includes solid state physics, nanoparticles, SEM.

E-mail: [esko\\_@ukr.net](mailto:esko_@ukr.net),

<https://orcid.org/0000-0001-8929-345X>

## Індуковане лазером теплове випромінювання вуглецевих мікрочастинок на прозорих тепловідвідних підкладках

К.С. Зеленська<sup>1</sup>, С.Є. Зеленський<sup>1\*</sup>, О.С. Колесник<sup>1</sup>, Toru Aoki<sup>2</sup>, П.О. Теселько<sup>1</sup>

**Анотація.** Теплове випромінювання є інформативним інструментом для дослідження властивостей матеріалів при високих температурах під дією лазерного опромінення. Досліджено кінетику загасання лазерно-індукованого теплового випромінювання мікрочастинок вуглецю, нанесених на тепловідвідні поверхні прозорих діелектриків (скла та сапфіру). Для збудження теплового випромінювання використовували YAG:Nd<sup>3+</sup> лазер з модуляцією добротності (тривалість імпульсу  $\tau_i = 20$  нс, густина енергії/потужності  $0.5 \text{ Дж}\cdot\text{см}^{-2}$ ,  $25 \text{ МВт}\cdot\text{см}^{-2}$ ). Розрахунки проведено на основі класичного рівняння теплопровідності. Зі збільшенням теплопровідності підкладки (від скла до сапфіру) спостерігалось зменшення тривалості імпульсу випромінювання.

**Ключові слова:** індуковане лазером теплове випромінювання, вуглецеві мікрочастинок, тепловідвідні підкладки.